JCB Report

Closed chromatin loops at the ends of chromosomes

Tatiana Nikitina and Christopher L. Woodcock

Biology Department, University of Massachusetts, Amherst, MA 01003

The termini of eukaryotic chromosomes contain specialized protective structures, the telomeres, composed of TTAGGG repeats and associated proteins which, together with telomerase, control telomere length. Telomere shortening is associated with senescence and inappropriate telomerase activity may lead to cancer. Little is known about the chromatin context of telomeres, because, in most cells, telomere chromatin is tightly anchored within the nucleus. We now report the successful release of telomere chromatin from chicken erythrocyte and mouse lymphocyte nuclei, both of which have a reduced karyoskeleton. Electron microscopy reveals telomere chromatin fibers in the form of closed terminal loops, which correspond to the "t-loop" structures adopted by telomere DNA. The ability to recognize isolated telomeres in their native chromatin conformation opens the way for detailed structural and compositional studies.

The Journal of Cell Biology

Introduction

The ends of linear eukaryotic chromosomes are capped by specialized DNA structures, the telomeres, that both protect against degradation and, together with telomerase, compensate for the shortening that occurs during each round of replication (Blackburn and Greider, 1995). Failure to properly regulate telomere length leads to the cessation of cell division or to cell death (Goytisolo and Blasco, 2002; Smogorzewska and de Lange, 2002). The absence of telomerase and consequent shortening of telomeres appears to be a normal and likely determining aspect of aging (Bodnar et al., 1998), and inappropriate telomerase activity is associated with many cancers (Blasco, 2003).

In addition to the terminal single-stranded DNA sequence, most telomeres contain several kilobases of double-stranded TTAGGG repeats. In mammals (Griffith et al., 1999), as well as *Trypanosoma brucei* (Munoz-Jordan et al., 2001), *Oxytricha fallax* (Murti and Prestcott, 1999), and *Pisum sativum* (Cesare et al., 2003), this repetitive DNA contributes to a unique "t-loop" sealed by an insertion of the single-stranded terminus into duplex DNA. Telomere chromatin contains nucleosomes but differs from bulk nuclear chromatin in having a nucleosome repeat length (NRL) that is ~40 bp shorter (Tommerup et al., 1994; Lejnine et al., 1995; Makarov et al., 1997), and has been predicted to induce a unique pattern of higher order folding (Fajkus and Trifonov, 2001). Intriguingly, in nuclei, telomere DNA occurs in distinct circles or rings (Luderus et al., 1996, Pierron and Puvion-Dutilleul, 1999). Telomeres are strongly anchored in nuclei, and remain with the insoluble "matrix" fraction after nuclease digestion (de Lange, 1992; Luderus et al., 1996).

The inability to extract native telomeres from nuclei effectively prevents the full examination and characterization of the unique higher order chromatin structure of these critical chromosomal components. We surmised that telomere anchoring to the insoluble nuclear matrix fraction, as reported by de Lange (1992) for HeLa cells, might be reduced in differentiated cells in which nuclei have a reduced complement of nonhistone chromosomal proteins. Here, we report the successful isolation of telomere chromatin from chicken erythrocytes and quiescent mouse lymphocytes, and show that the native interphase conformation is a closed chromatin loop.

Results and discussion

We selected avian erythrocytes and quiescent mammalian lymphocytes as sources of nuclei in which telomeres might be less strongly anchored to the nuclear matrix than in HeLa cells (de Lange, 1992; Luderus et al., 1996). Chicken erythrocyte nuclei have a much reduced complement of non histone chromosomal proteins and very little internal nuclear matrix (Lafond and Woodcock, 1983), whereas quiescent lymphocytes have small nuclei packed with compact heterochromatin, and very little cytoplasm (Setterfield et al., 1983). Nuclei from chicken erythrocytes and mouse spleen lymphocytes were isolated and digested with a mixture of seven frequent cutter restriction endonucleases (REs), which do not attack

Address correspondence to Christopher L. Woodcock, Biology Dept., University of Massachusetts, Amherst, MA 01003. Tel.: (413) 545-2602. Fax: (413) 545-3243. email: chris@bio.umass.edu

Key words: telomere; chromatin; electron microscopy; TRF1

Abbreviations used in this paper: RE, restriction endonuclease; NRL, nucleosome repeat length.

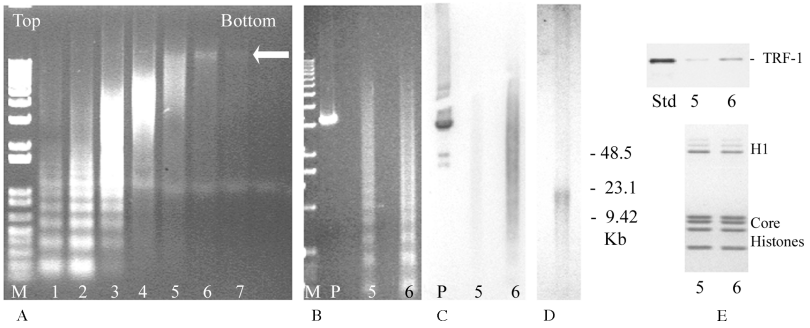

Figure 1. **Telomere DNA is enriched in rapidly sedimenting chromatin after restriction enzyme digestion.** (A) Ethidium bromide-stained agarose gel of DNA from sucrose gradient fractions. M, DNA size marker; arrow indicates the high molecular weight component shown to be enriched in telomere sequences. (B and C) Chromatin from fractions 5 and 6 was redigested with micrococcal nuclease, and the DNA purified and separated on agarose, together with a plasmid containing ~300 tandem repeats of telomere DNA. (B) Ethidium bromide stain. (C) Southern blot with telomere probe. Fraction 6 is highly enriched in telomere DNA. M, DNA size marker; P, plasmid DNA standard. (D) Telomere enriched chromatin contains the expected size range of telomere DNA. Southern blot of DNA from telomere-enriched fraction 6 (A) separated by pulsed field gel electrophoresis and probed with telomere DNA. (E) Exogenous hTRF1 binds preferentially to the telomere-enriched chromatin fraction. hTRF1 was added to RE-solubilized chromatin before sucrose gradient centrifugation. Total protein from gradient fractions 5 and 6 (A) were separated on SDS-PAGE and Western blotted with anti-hTRF1. Top panel shows blot that includes an hTRF1 standard (Std). Bottom panel verifies approximately equal loading of chromatin as judged by Coomassie blue stain intensity of core histones on a duplicate gel.

the telomere repeat sequence. The fraction of total telomere DNA solubilized was then measured by dot blot hybridization with a labeled telomere DNA probe. Approximately 50% of telomeric DNA was released from chicken erythrocyte nuclei and 25% from quiescent lymphocyte nuclei under these conditions. After RE digestion and release, soluble chromatin was separated on sucrose gradients, and the DNA was extracted from each fraction and separated on agarose gels (Fig. 1 A). To estimate the proportion of telomere sequence in each fraction, the chromatin was briefly redigested with micrococcal nuclease and then hybridized with a telomere probe. A plasmid containing a known quantity of telomere DNA provided an internal quantitation standard (Fig. 1, B and C). The blots showed that maximal enrichment in telomere chromatin occurs in the most rapidly sedimenting fractions, and quantitation of the hybridization signal indicates that 10–20% of fraction 6 consists of telomere chromatin. Pulsed field gel electrophoresis of DNA isolated from maximally enriched fractions indicates a modal telomere size of ~20 kb for chicken erythrocytes (Fig. 1 D), similar to that of telomere DNA in the total RE digest.

Electron microscopic examination of telomere-enriched chromatin after fixation in 5–75 mM monovalent ions reveal, in addition to linear fibers, highly distinct structures consisting of a closed loop and a "tail" (Fig. 2). Both the linear and looped chromatin fibers have an irregular diameter ranging from ~10 to ~30 nm depending on the ionic strength. To test the hypothesis that the loops represented telomeres, we used TRF1, a telomere binding protein which binds specifically to TTAGGG sequences (Chong et al., 1995; Bianchi et al., 1997, 1999). Purified recombinant human TRF1 (hTRF1) was biotinylated, allowing its presence to be detected after exposure to streptavidin-gold marker beads. We verified that this probe, which contains two to three biotins per molecule, was able to decorate the telomere portion of a DNA plasmid composed of vector and ~300 bp of tandem TTAGGG repeats (provided by J.D. Griffith, University of North Carolina, Chapel Hill, NC), and that streptavidin-gold beads bound specifically to the decorated portion (unpublished data). Biotinylated hTRF1 was then mixed with RE-solubilized nuclear chromatin from chicken erythrocyte nuclei, and fractionated on sucrose gradients. Subsequent Western blotting with an anti-TRF1 antibody showed that the biotinylated probe bound preferentially to the fractions enriched in telomere DNA (Fig. 1 E). Electron microscopic examination revealed gold beads primarily on the loops (Fig. 3 A), with a highly significant ($P < 0.0001$)

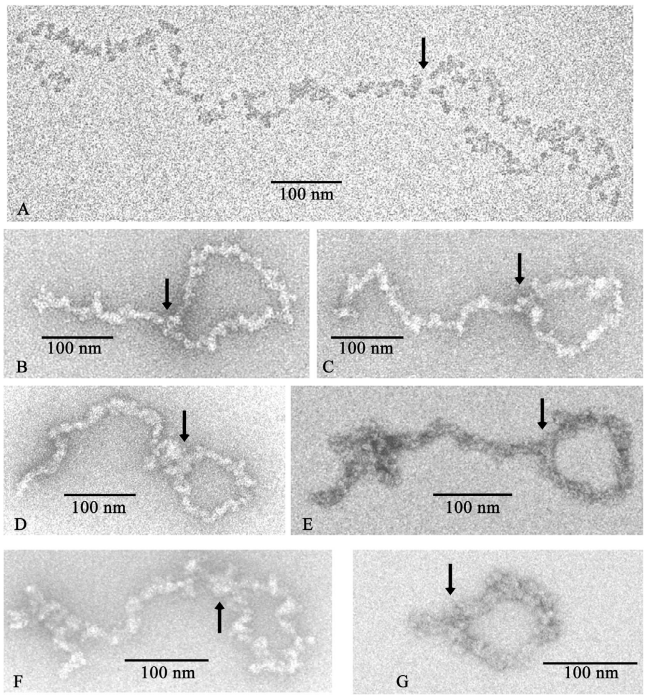

Figure 2. **Telomere-enriched chromatin contains conspicuous loop–tail structures.** Chromatin was fixed mildly with glutaraldehyde in 5 mM NaCl (A), 25 mM NaCl (B and C) or 75 mM NaCl (D–G) and either positively stained with phosphotungstic acid (A) or negatively stained with uranyl acetate (B–G). In 5 mM NaCl, the chromatin assumes an open "beads-on-a-string" conformation, and compacts to yield typical "30-nm" fibers with increased ionic strength. Arrows denote putative loop–tail junctions. A–E are from chicken erythrocyte preparations; F and G are from mouse spleen lymphocytes.

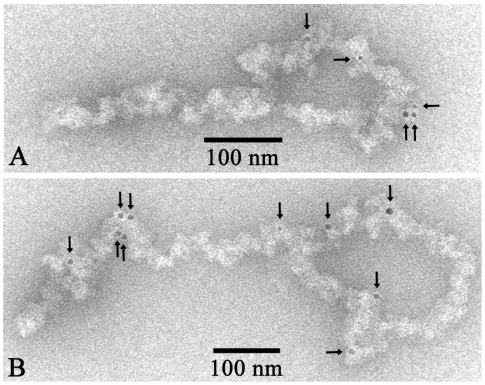

Figure 3. **Chromatin loops contain telomeric DNA.** After exposure of RE-solubilized chicken erythrocyte chromatin to biotinylated hTRF1 and streptavidin-gold, beads (arrows) are seen primarily on loops, where they tend to be randomly distributed (A). Occasionally, a cluster of beads occurs on tails (B). Statistical analysis shows a highly significant ($P < 0.0001$) preference of gold beads for loops over tails.

preference for loops over tails, although occasionally, a cluster of gold particles was seen on tails (Fig. 3 B). The presence of gold-free tails after extensive RE digestion is probably attributable to the repetitive nature and low frequency of RE sites in subtelomere DNA. Controls in which telomere chromatin was exposed to streptavidin gold without prior hTRF1 treatment were virtually gold free (unpublished data). Loops were ~10-fold less frequent in chromatin of similar size generated by micrococcal nuclease (unpublished data) showing that loop formation is not simply a property of very long chromatin fibers. The labeling pattern observed with TRF1 is unlikely to be due to preferential, but not telomere-related binding to fraction 6 chromatin. This is demonstrated by the distribution of BSA, a component of RE buffers that, unless released, adheres nonspecifically to chromatin (see Materials and methods), and is present in all gradient fractions in proportion to chromatin content (unpublished data). Together, these results clearly demonstrate that the loops represent telomere chromatin, and are thus the native chromatin equivalents of the loops observed in isolated telomeric DNA (Griffith et al., 1999).

Telomere-enriched fractions typically contained ~25% loops and 75% linear chromatin fibers sufficiently long to form loops. Linear chromatin could be generated in several ways: nontelomeric chromatin with no RE sites (or no exposed sites), telomeres in a nonlooped configuration, looped telomeres in which the loop has been opened during preparation, and chromatin from interstitial telomere sequences which are common in chicken (Nanda and Schmid, 1994). In view of the multiple potential origins of linear fibers, we confined our analysis of gold bead distributions to looped chromatin.

Telomere loops from chicken erythrocyte nuclei in 75 mM NaCl varied in contour length from ~200 to ~600 nm, with a mean of 317 nm (Fig. 4). Telomere DNA with a modal length of ~20 kb (Fig. 1 D), would require a nucleosome packing ratio of ~1:20 to yield a 317 nm length of chromatin fiber. This is somewhat lower than the ~1:30 packing ratio measured for bulk chromatin from these nuclei under similar ionic conditions (Woodcock et al., 1984; Gerchman and Ramakrishnan, 1987), suggesting a lower level of compaction for telomere chromatin. Like bulk chromatin, telomeres appeared in an open beads-on-a-string conformation at low ionic strength (Fig. 2 A), and rough counts of the number of nucleosomes in the loops (75–150) also indicate a DNA loop size in the 15–30 kb range. Fibers which respond to changes in ionic strength by varying in diameter (and compaction) are characteristic of histone H1-containing chromatin (Widom, 1989), supporting the suggestion that telomere chromatin contains H1 (Bedoyan et al., 1996).

We did not observe the columnar stacking of nucleosomes predicted for short nucleosome repeat telomere chromatin (Fajkus and Trifonov, 2001) or any other consistent differences in fiber diameter or morphology between telomere loops and tails or between loops and linear fibers that might be attributed to the ~40-bp reduction in NRL for telomere chromatin nuclei (Lejnine et al., 1995). Also, there was no apparent change in fiber morphology close to the loop–tail junction as might be expected for telomeres with a highly irregular nucleosome organization close to the terminus (Tommerup et al., 1994).

Studies of the location of telomere repeats in HeLa nuclei in which telomere DNA ranges in size from 14 to 31 kb have identified discrete circular or ring-shaped structures ~120 nm in diameter (Luderus et al., 1996; Pierron and Puvion-Dutilleul, 1999), which persist in nuclear matrix preparations and are presumed to represent the native telomere chromatin conformation at in vivo anchorage sites. The close correspondence in contour length between the perimeter of these sites (~375 nm) and the chromatin loops observed here (Fig. 4) suggests that they may represent in situ and in vitro manifestations of the same structure. The retention in nuclear matrix preparations of TRF1 as well as telomere chromatin has led to the hypothesis that TRF1 has an anchoring function (Luderus et al., 1996), and it is perhaps significant in this respect that we find the chicken homologue of TRF1 (De Rycker et al., 2003) to be undetectable in chicken erythrocyte nuclei under Western blotting conditions that give a strong signal from chicken liver nuclei. Similarly, using an antibody against mouse TRF1, we

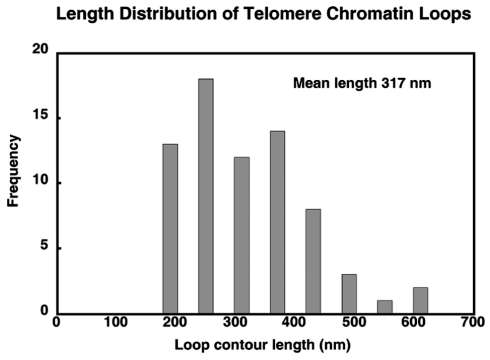

Figure 4. **Distribution of loop lengths ($n = 71$) for telomere chromatin from chicken erythrocyte nuclei fixed in 75 mM NaCl.**

were able to detect the protein in nuclei from cycling 3T3 fibroblasts and mouse ES cells, but not from quiescent lymphocytes (unpublished data), although TRF1 mRNA has been detected in this tissue (Broccoli et al., 1997). Luderus et al. (1996) noted that a small fraction of TRF1-depleted telomeric chromatin could be released from HeLa nuclei, and suggested that telomeres might be transiently released from their anchorage sites. The present data confirm the lack of TRF1 in RE-solubilized telomeric chromatin, and further suggest that TRF1 abundance in nuclei is correlated with cell proliferation and telomere anchoring.

TRF1 plays an important role in telomere length control (van Steensel and de Lange, 1997; Smogorzewska et al., 2000), in conjunction with tankyrase, TIN1 and POT1 acting to repress telomerase activity in cycling cells (Loayza and de Lange, 2003). At present, the implications of the low abundance of TRF1 in quiescent cells are unclear, although as there is little or no detectable telomerase activity in unstimulated lymphocytes (Liu et al., 2001), it is possible that TRF1-mediated regulation is not needed. As shown here, TRF1 will bind stably and specifically to telomeric chromatin in vitro (Fig. 1 E), and, in light of its ability to bend DNA (Bianchi et al., 1997, 1999) and induce side-by-side DNA pairing (Griffith et al., 1998), it will be interesting to examine in detail any changes in chromatin morphology accompanying TRF1 binding.

It has been suggested that a primary function of DNA t-loops is to protect the chromosome end from recognition as a breakpoint by DNA repair machinery (Griffith et al., 1999), and in this context, the histone association and compaction afforded by chromatin is likely to enhance the protective role. The distinct morphology of telomeres reported here will allow detailed structural and compositional studies of these essential chromosome components. It will be particularly important to investigate the relationship between NRL and fiber architecture, and the 3D chromatin organization at the loop–tail junction where the single-stranded terminus is inserted.

Materials and methods

Nuclei were prepared from chicken erythrocytes and mouse splenocytes as described previously (Grigoryev et al., 1992; Fan et al., 2003), and stored at −80°C in 10 mM NaCl, 3 mM $MgCl_2$, 10 mM Tris, pH 7.4, containing 50% glycerol. 0.2 mM PMSF was present throughout the preparation, and protease inhibitor cocktail (Sigma-Aldrich) was included at the homogenization step. Nuclei containing ~3 mg DNA were digested with CfoI, HaeIII, HinfI, MspI, and RsaI (Promega Corp.) at a concentration of 0.5 to 1.0 U/1 μg of DNA in 50 mM NaCl, 6 mM $MgCl_2$, 1 mM DTT, 6 mM Tris, pH 7.5, with 0.5 mM PMSF for 4 h at 37°C. Preparations were then dialyzed overnight against 5 mM NaCl, 10 mM Tris, pH 7.5, at 4°C, followed by a second round of RE digestion with BamHI and EcoRI (Promega) for 2 h at 37°C in 0.3 mM $MgCl_2$, 50 mM NaCl, 1 mM DTT, 10 mM Tris, pH 7.5. The reaction was stopped with 1 mM EDTA, held for 30 min at 0°C, then centrifuged for 5 min at 800 *g*. Recovery of telomere chromatin was estimated by comparing dot blots of purified DNA from total nuclei and RE-solubilized chromatin. Samples were applied to Hybond-N+ membranes (Amersham Biosciences), and baked for 2 h at 80°C. Membranes were probed with a 36-bp telomere DNA probe labeled with the Alkphos Direct Labeling reagent and the signal visualized using the CDP-Star detection system (Amersham Biosciences) on Hyperfilm ECL according to the manufacturer's directions. For sucrose gradient analysis, the BSA present in the enzyme stocks (which tends to adhere to chromatin), was released by bringing the soluble chromatin to 75 mM NaCl and 0.1% NP-40 and holding at 0°C for 10 min before layering onto 5–40% sucrose gradients containing 25 mM NaCl, 0.2 mM EDTA, 5 mM Hepes, pH 7.5. Gradients were centrifuged for 75 min at 32,000 rpm in an SW41 rotor (Beckman Instruments) and 1-ml fractions were collected.

DNA extracted from fractions was separated on 1% agarose gels and stained with ethidium bromide. Selected fractions were dialyzed against 25 mM NaCl, 1 mM EDTA, 5 mM Hepes, pH 7.5, and concentrated using 100,000 MW cutoff Centricon units (Amicon Inc.). To examine telomere enrichment, chromatin fractions were briefly digested with micrococcal nuclease (1.5 U of enzyme per 1 mg DNA for 5 min at 20°C in 1 mM $CaCl_2$, 1 mM PMSF, 10 mM Tris, pH 7.5) to provide a size range convenient for transfer and blotting. DNA was then extracted, separated on 1% agarose gels, transferred to membranes and Southern blots with a telomere probe performed as described for dot blots. To examine the DNA size distribution of telomere DNA, fractions were separated by pulsed field gel electrophoresis on 1% FastLane agarose (FMS BioProducts), at 6 V/cm for 15 h with an excluded angle of 120° in 45 mM sodium borate, 1.0 mM EDTA, 45 mM Tris, pH 8.3, together with low range PFG Marker (New England Biolabs, Inc.) for DNA size calibration. To facilitate transfer of high MW DNA, gels were treated with 0.25 M HCl for 60 min, rinsed with H_2O, and treated with 0.5 M NaOH, 1.5 M NaCl for 30 min before neutralizing in 1.5 M NaCl, 1 M Tris-HCl, pH 7.4, and probing for telomere sequences as described above.

For EM, concentrated samples were equilibrated to the desired NaCl concentration and fixed with 0.1% glutaraldehyde for 4 h, before applying to glow-discharged carbon films and staining with aqueous uranyl acetate or alcoholic phosphotungstic acid (Woodcock and Horowitz, 1998). Grids were examined in a FEI Tecnai 12 Transmission EM at 100KV with LaB6 filament, and micrographs recorded with a 2048 × 2048 CCD camera (TVIPS). Images were typically recorded in a 16-bit TIFF format. Contour lengths were measured on unprocessed images using the ImageJ image processing suite. For presentation purposes, images were converted to 8-bit TIFF files in ImageJ, and cropping and adjustment of contrast and brightness performed with FotoCanvas v 1.1 (ACD Systems, Ltd.).

hTRF1 was prepared in Sf21 cells (provided by J. Burand, University of Massachusetts) from a baculovirus plasmid (provided by T. de Lange, The Rockefeller University, New York, NY) containing the His-tagged gene (Chong et al., 1995), purified using the TALON affinity resin system (BD Biosciences) according to the manufacturer's directions, and stored in 500 mM KCl, 0.2 mM PMSF, 20 mM Hepes, pH 7.5, with 20% glycerol at −80°C. hTRF1 was biotinylated using the NHS-PEO-biotin reagent (Pierce Chemical Co.) according to the manufacturer's recommendations. The extent of biotinylation was measured using the EZ Biotin Quantitation Kit (Pierce Chemical Co.). RE-digested chromatin was mixed with biotinylated hTRF1 (hTRF1-bio) at a ratio of 16 μg hTRF1-bio to 1 μg telomere DNA (assuming telomere DNA constitutes 0.2% of total chicken erythrocyte DNA; Lejnine et al., 1995) for 30 min at 37°C followed by 1 h at 0°C, before separation on sucrose gradients as described above. Chromatin fractions enriched in telomeric sequence were fixed briefly in 75 mM NaCl, applied to glow-discharged carbon films, rinsed, and the grids floated on a drop of 5-nm streptavidin-gold beads (Electron Microscopy Supplies) for 5 min before rinsing with H_2O and staining. Micrographs of loop–tail structures were analyzed by dividing each loop or tail into 50-nm segments, and the number of gold beads on each segment recorded. These values for 71 loops and tails were subjected to a nonpaired *t* test to determine the probability that loops and tails had identical bead distributions. PSI-Plot v. 7.0 (Poly Software International) was used for statistical analysis and histogram plotting. To determine the distribution of hTRF1 in the gradients, fractions were dialyzed and concentrated, aliquots solubilized in SDS-sample buffer, separated by SDS-PAGE, and the proteins electrophoretically transferred to membranes. Membranes were probed with anti-TRF1 (Imgenex) and the blots developed with the ECL system (Amersham Biosciences). Stained gels and developed films were recorded and analyzed using the Gel-Doc system and Quantity 1 software (Bio-Rad Laboratories). To examine the relative abundance of TRF1 in nuclei and RE-solubilized chromatin, Western blots were probed for chicken TRF1 with a specific antibody (De Rycker et al., 2003) supplied by C.M. Price (University of Cincinnati, Cincinnati, OH), and for mouse TRF1 with an antibody purchased from Alpha Diagnostics Inc. For all Western blots, the loading of chromatin was adjusted to be constant by staining duplicate lanes with Coomassie blue and recording the stain intensity of the core histones.

We thank D. Staynov for helpful discussions, T. de Lange for a baculovirus construct containing TRF1, J.D. Griffith for a bacterial plasmid containing tandem TTAGGG repeats, C.M. Price for antibody to cTRF1, and J. Burand for SF21 cells and assistance with baculovirus preparations.

This work was supported in part by National Institutes of Health GM43786 to C.L. Woodcock.

Submitted: 22 March 2004
Accepted: 3 June 2004

References

Bedoyan, J.K., S. Lejnine, V.L. Makarov, and J.P. Langmore. 1996. Condensation of rat telomere-specific nucleosomal arrays containing unusually short DNA repeats and histone H1. *J. Biol. Chem.* 271:18485–18493.

Bianchi, A., S. Smith, L. Chong, P. Elias, and T. de Lange. 1997. TRF1 is a dimer and bends telomeric DNA. *EMBO J.* 16:1785–1794.

Bianchi, A., R.M. Stansel, L. Fairall, J.D. Griffith, D. Rhodes, and T. de Lange. 1999. TRF1 binds a bipartite telomeric site with extreme spatial flexibility. *EMBO J.* 18:5735–5744.

Blackburn, E.H., and C.W. Greider. 1995. Telomeres. Cold Spring Harbor Laboratory Press, Cold Spring Harbor, NY. 396 pp.

Blasco, M.A. 2003. Telomeres and cancer: a tale with many endings. *Curr. Opin. Genet. Dev.* 13:70–76.

Bodnar, A.G., M. Ouellette, M. Frolkis, S.E. Holt, C.P. Chiu, G.B. Morin, C.B. Harley, J.W. Shay, S. Lichtenstainer, and W.E. Wright. 1998. Extension of life-span by introduction of telomerase into normal human cells. *Science.* 279:349–352.

Broccoli, D., L. Chong, S. Oelmann, A.A. Fernald, N. Marziliano, B. van Steensel, D. Kipling, M.M. Le Beau, and T. de Lange. 1997. Comparison of the human and mouse genes encoding the telomeric protein, TRF1: chromosomal localization, expression and conserved protein domains. *Hum. Mol. Genet.* 6:69–76.

Cesare, A.J., N. Guinney, S. Wilcox, D. Subrimanain, and J.D. Griffith. 2003. Telomere looping in *P. sativum* (common garden pea). *Plant J.* 36:271–279.

Chong, L., B. van Steensel, D. Broccoli, H. Erdjument-Bromage, J. Hanish, P. Tempest, and T. de Lange. 1995. A human telomeric protein. *Science.* 270: 1663–1667.

de Lange, T. 1992. Human telomeres are attached to the nuclear matrix. *EMBO J.* 11:717–724.

De Rycker, M., R.N. Venkatesan, C. Wei, and C.M. Price. 2003. Vertebrate tankyrase domain structure and sterile a motif (SAM)-mediated multimerization. *Biochem. J.* 372:87–96.

Fajkus, J., and E.N. Trifonov. 2001. Columnar packing of telomeric nucleosomes. *Biochem. Biophys. Res. Commun.* 280:961–963.

Fan, Y., T. Nikitina, M. Morin-Kensicki, J. Zhao, T.R. Magnusen, C.L. Woodcock, and A.I. Skoultchi. 2003. H1 linker histones are essential for mouse development and affect nucleosome spacing in vivo. *Mol. Cell. Biol.* 23: 4559–4572.

Gerchman, S.E., and V. Ramakrishnan. 1987. Chromatin higher order structure studied by neutron scattering and scanning transmission electron microscopy. *Proc. Natl. Acad. Sci. USA.* 84:7802–7806.

Goytisolo, F.A., and M.A. Blasco. 2002. Many ways to telomere dysfunction: in vivo studies using mouse models. *Oncogene.* 21:584–591.

Griffith, J., A. Bianchi, and T. de Lange. 1998. TRF1 promotes parallel pairing of telomeric tracts in vitro. *J. Mol. Biol.* 278:79–88.

Griffith, J.D., L. Comeau, S. Rosenfiel, R.M. Stansel, A. Bianchi, H. Moss, and T. de Lange. 1999. Mammalian telomeres end in a large duplex loop. *Cell.* 97: 503–514.

Grigoryev, S.A., V.O. Solovieva, K.S. Spirin, and I.A. Krasheninnikov. 1992. A novel nonhistone protein (MENT) promotes nuclear collapse at the terminal stage of avian erythropoiesis. *Exp. Cell Res.* 198:268–275.

Lafond, R.E., and C.L. Woodcock. 1983. Status of the nuclear matrix in mature and embryonic chick erythrocyte nuclei. *Exp. Cell Res.* 147:31–39.

Lejnine, S., V.L. Markov, and J.P. Langmore. 1995. Conserved nucleoprotein structure at the ends of vertebrate and invertebrate chromosomes. *Proc. Natl. Acad. Sci. USA.* 92:2393–2397.

Liu, K., R.J. Hodes, and N. Weng. 2001. Telomerase activation in human T lymphocytes does not require increase in telomerase reverse transcriptase (hTERT) protein but is associated with hTERT phosphorylation and nuclear translocation. *J. Immunol.* 166:4826–4830.

Loayza, D., and T. de Lange. 2003. POT1 as a terminal transducer of TRF1 telomere length control. *Nature.* 423:1013–1018.

Luderus, M.E.E., B. van Steensel, L. Chong, O.C.M. Sibon, F.F.M. Cremers, and T. de Lange. 1996. Structure, subnuclear distribution, and nuclear matrix association of the mammalian telomeric complex. *J. Cell Biol.* 135:867–881.

Makarov, V., Y. Hirose, and J.P. Langmore. 1997. Long G-tails at both ends of human chromosomes suggest a C-strand degradation mechanism for telomere shortening. *Cell.* 88:657–666.

Munoz-Jordan, J.L., G.A.M. Cross, T. de Lange, and J.D. Griffith. 2001. t-loops at trypanosome telomeres. *EMBO J.* 20:579–588.

Murti, K.D., and D.M. Prestcott. 1999. Telomeres of polytene chromosomes in a ciliated protozoan terminate in duplex DNA loops. *Proc. Natl. Acad. Sci. USA.* 96:14436–14439.

Nanda, I., and M. Schmid. 1994. Localization of the telomeric (TTAGGG)n sequence in chicken (*Gallus domesticus*) chromosomes. *Cytogenet. Cell Genet.* 65:190–193.

Pierron, G., and F. Puvion-Dutilleul. 1999. An anchorage nuclear structure for telomeric repeats in HeLa cells. *Chromosome Res.* 7:581–592.

Setterfield, G., R. Hall, T. Bladon, J. Little, and J.G. Kaplan. 1983. Changes in structure and composition of lymphocyte nuclei during mitogenic stimulation. *J. Ultrastruct. Res.* 82:264–282.

Smogorzewska, A., and T. de Lange. 2002. Different telomere damage signaling pathways in human and mouse cells. *EMBO J.* 21:4338–4348.

Smogorzewska, A., B. van Steensel, A. Bianchi, S. Oelmann, M.R. Schaefer, G. Schnapp, and T. de Lange. 2000. Control of telomere length by TRF1 and TRF2. *Mol. Cell. Biol.* 20:1659–1668.

Tommerup, H., A. Dousmanis, and T. de Lange. 1994. Unusual chromatin in human telomeres. *Mol. Cell. Biol.* 14:5777–5785.

van Steensel, B., and T. de Lange. 1997. Control of telomere length by the human telomere protein TRF1. *Nature.* 385:740–743.

Widom, J. 1989. Toward a unified model of chromatin folding. *Annu. Rev. Biophys. Biophys. Chem.* 18:365–395.

Woodcock, C.L., and R.A. Horowitz. 1998. Electron microscopy of chromatin with nucleosomal resolution. *Methods Cell Biol.* 53:167–186.

Woodcock, C.L., L.-L.Y. Frado, and J.B. Rattner. 1984. The higher order structure of chromatin: evidence for a helical ribbon arrangement. *J. Cell Biol.* 99: 42–52.